

Characterization of the Mechanism of Interaction Between α_1 -Acid Glycoprotein and Lipid Membranes by Vacuum-Ultraviolet Circular-Dichroism Spectroscopy

Koichi Matsuo^[a], Munehiro Kumashiro^[b], and Kunihiro Gekko^[a]

Abstract: α_1 -Acid glycoprotein (AGP) interacts with lipid membranes as a peripheral membrane protein so as to decrease the drug-binding capacity accompanying the $\beta \rightarrow \alpha$ conformational change that is considered a protein-mediated uptake mechanism for releasing drugs into membranes or cells. This study characterized the mechanism of interaction between AGP and lipid membranes by measuring the vacuum-ultraviolet circular-dichroism (VUVCD) spectra of AGP down to 170 nm using synchrotron radiation in the presence of five types of liposomes whose constituent phospholipid molecules have different molecular characteristics in the head groups (e.g., different net charges). The VUVCD analysis showed that the α -helix and β -strand contents and the numbers of segments of AGP varied with the constituent phospholipid molecules of liposomes, while combining VUVCD data with a neural-network method predicted

that these membrane-bound conformations comprised several common long helix and small strand segments. The amino-acid composition of each helical segment of the conformations indicated that amphiphilic and positively charged helices formed at the N- and C-terminal regions of AGP, respectively, were candidate sites for the membrane interaction. The addition of 1 M sodium chloride shortened the C-terminal helix while having no effect on the length of the N-terminal one. These results suggest that the N- and C-terminal helices can interact with the membrane via hydrophobic and electrostatic interactions, respectively, demonstrating that the liposome-dependent conformations of AGP analyzed using VUVCD spectroscopy provide useful information for characterizing the mechanism of interaction between AGP and lipid membranes.

Keywords: α_1 -acid glycoprotein; electrostatic and hydrophobic interactions; membrane-bound conformation; secondary structure of protein; synchrotron radiation circular dichroism

Introduction

In addition to the integral membrane proteins,^{1–3} the nonintegral membrane proteins such as peripheral membrane proteins have crucial biological functions such as toxin penetration, electron transport, and amyloid fibril formation.^{4–6} In the case of peripheral membrane proteins, it is known that a water-soluble protein approaches to and interacts with the surface of membrane to induce large structural changes accompanying the expression of its unique functions.^{4–6} α_1 -Acid glycoprotein (AGP) is a peripheral membrane protein that exhibits characteristic abilities to bind to numerous basic, acidic, and neutral drugs as well as to steroid hormones in the native (N) state.^{7, 8} However, this binding capacity decreases due to interactions with the membrane that induce the $\beta \rightarrow \alpha$ conformational change. Thus, AGP has been studied as a model protein capable of delivering drugs into a membrane or cell.^{9, 10}

AGP (pI=2.8–3.8) is a polypeptide consisting of 183 amino acids that includes 5 glycan chains linked to Asn residues (Asn-15, -38, -54, -75, and -85)^{11, 12} accounting for about 40% of its total mass of 36 kDa.¹³ The three-dimensional structure of AGP with glycan chains has not been resolved, but X-ray crystallography has revealed that unglycosylated human recombinant AGP has a β -barrel conformation, as shown in Figure 1.¹⁴ However, since the peripheral membrane proteins such as membrane-bound AGP are not amenable to X-ray crystallography and nuclear magnetic resonance (NMR) spectroscopy,¹⁵ the tertiary structure of AGP in the membrane has not been characterized.

Knowledge of both the secondary and tertiary structures of proteins is useful for understanding their structure–function relationships. The secondary structure of AGP in the N state has been investigated using circular dichroism (CD), Raman, and Fourier-transform infrared

spectroscopy to reveal the binding sites of drugs and the structure–function relationships of AGP.^{9, 16–21} CD spectroscopy has been used to analyze the structure of AGP in lipid membranes because it is very sensitive to local peptide structures and applicable to any size of protein at a low concentration under various experimental conditions, such as in the presence of a membrane.²² Nishi et al. measured the CD spectrum of AGP from 250 to 200 nm in reverse micelles and phosphatidylglycerol (PG) liposome in a mildly acidic condition (pH 4.5), and confirmed that the β -barrel structure of AGP transformed to the α -helix-rich conformation.^{9, 16} In experiments using Trp and His mutants those authors also found that W25, W160, and H172 were key sites for interacting with the liposome (Figure 1).^{16, 23} Vacuum-ultraviolet CD (VUVCD) spectroscopy using synchrotron radiation as a light source extended the wavelength range of the CD measurements of AGP down to the VUV region (~160 nm) and

[a] Koichi Matsuo and Kunihiro Gekko
Hiroshima Synchrotron Radiation Center
Hiroshima University
Higashi-Hiroshima 739-0046, Japan
Phone: +81-82-424-6423
Fax: +81-82-424-6424
E-mail: pika@hiroshima-u.ac.jp

[b] Munehiro Kumashiro
Department of Physical Science
Graduate School of Science, Hiroshima University
1-3-1 Kagamiyama, Higashi-Hiroshima, Hiroshima 739-8526, Japan

Received: ((will be filled in by the editorial staff))

Revised: ((will be filled in by the editorial staff))

Published online: ((will be filled in by the editorial staff))

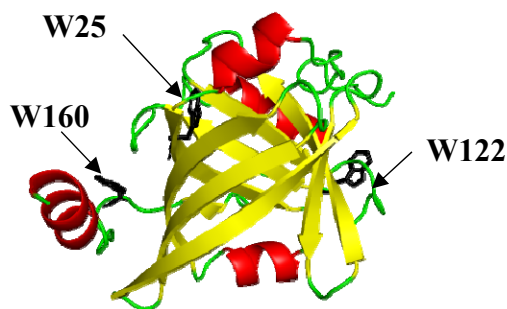


FIGURE 1 Crystal structure of unglycosylated human recombinant AGP (PDB code: 3kq0), which comprises four α -helix and nine β -strand segments. The types of secondary structures were determined using the DSSP method⁴¹ in which the 3_{10} -helices are assigned as unordered structures. The positions of W25, W122, and W160 are indicated.

allowed us to accurately estimate the secondary-structure contents and numbers of segments in the PG liposome.^{24–26} These secondary-structure parameters were combined with a neural network (NN) (VUVCD-NN) method to characterize the positions of secondary structures of the membrane-bound conformation of AGP. The findings suggested that the N-terminal helix including W25 and the C-terminal helix including W160 and H172 can interact with the surface of PG liposome.²⁶ However, the mechanism of interaction between AGP and lipid membranes remains controversial because the membrane-bound conformation of AGP has been analyzed only in the presence of PG liposome, whereas the conformation depends on the constituent phospholipid molecules of liposomes,^{27, 28} while the roles of the two helical regions predicted as the membrane interaction sites have not been fully considered.

This study characterized the membrane interaction sites and the mechanism of interaction between AGP and lipid membranes by applying VUVCD spectroscopy to the conformation analysis of AGP in the presence of five types of liposomes. The constituent phospholipid molecules of the liposomes are major components of human cells²⁹ and have different molecular characteristics in the head groups (e.g., different net charges), giving unique properties to the liposome surface. The secondary structures of different membrane-bound conformations of AGP according to the types of liposomes were characterized at the amino-acid sequence level, and the interaction mechanism was investigated in terms of hydrophobic and electrostatic interactions.

Materials and Methods

2.1 Materials

AGP from human plasma (Cohn fraction VI) was purchased from Sigma (St. Louis, MO) and used without further purification because gel electrophoresis showed the presence of single major band. Dimyristoyl phosphatidylcholine (DMPC), sphingomyelin (SM), dimyristoyl phosphatidylethanolamine (DMPE), dimyristoyl phosphatidylserine (DMPS), and phosphatidylinositol (PI), which are major membrane components of human cells, were obtained from Avanti (Alabaster, AL).²⁹ Their chemical structures are shown in Figure S1. All of these phospholipid molecules had purities of >98%,

and were used without further purification. AGP was dissolved in 20 mM sodium phosphate buffer (pH 7.4) or in 20 mM sodium acetate buffer (pH 4.5), and the solutions were exhaustively dialyzed against the same buffer at 4°C. The dialyzed protein solutions were centrifuged at 14,000 rpm for 15 min and filtered by a membrane with a pore size of 20 μ m (DISMIC 25AS020AS, ADVANTEC, Tokyo) to remove aggregates. The AGP concentration was determined by measuring the absorption (V-560, Jasco, Tokyo) using the molar extinction coefficient of 33,074 $M^{-1} cm^{-1}$ which was estimated from extinction coefficient of 8.93 dL (g cm^{-1}) at 278 nm¹⁶ and total mass of AGP. This molar extinction coefficient was close to that calculated from the amino-acid sequence of AGP (33,140 $M^{-1} cm^{-1}$ at 280 nm).³⁰

2.2 Liposome preparation

The DMPC, SM, DMPE, DMPS, and PI liposomes were prepared as described previously.^{9, 26} All of the phospholipids were dispersed in 20 mM sodium acetate buffer (pH 4.5) above the phase-transition temperature of the phospholipid: 24°C for DMPC, \approx 40°C for SM, 50°C for DMPE, 35°C for DMPS, and \approx 0°C for PI.^{31–33} The phospholipid solutions in the sample vial were placed alternately in liquid nitrogen and a heated block for three to five freeze/thaw cycles in order to enhance the hydration of the lipid. Small unilamellar vesicles were prepared using the extrusion technique: the lipid solutions were passed 25 times through a polycarbonate membrane with a pore size of 100 nm above the phase-transition temperature to make them optically clear. The liposome vesicles were mixed with protein solution at final concentrations of 50 μ M protein and 3 mM phospholipid (i.e., molar ratio of protein to phospholipid of 1:60).^{9, 26} The protein–liposome mixtures were incubated at room temperature overnight before performing the VUVCD measurements.

2.3 VUVCD measurements

The VUVCD spectra of AGP in the presence or absence of liposomes were measured from 260 to 170 nm using the VUVCD spectrophotometer in the Hiroshima Synchrotron Radiation Center and an assembled-type optical cell at 25°C. The optical devices and sample cell of the spectrophotometer are described in detail elsewhere.^{34, 35} The path length of the optical cell was adjusted with a Teflon spacer to 10.6 μ m. All of the VUVCD spectra were recorded with a 1.0-mm slit, a 4-s time constant, a 20-nm min^{-1} scan speed, and using four to nine accumulations. The optical cell was located within 10 mm of the photomultiplier so as to minimize the effects of light scattering from the liposome particles.^{36, 37}

2.4 Secondary-structure analysis

The secondary structures of proteins in the presence or absence of liposomes were analyzed using the SELCON3 program^{38, 39} and the database of VUVCD spectra of 31 reference proteins with known X-ray structures.^{24, 25} These reference proteins are water-soluble, but they would be suitable for liposome-bound systems because there was no evidence of wavelength shifts between the CD spectra of soluble and membrane proteins.⁴⁰ However, the $n-\pi^*$ and $\pi-\pi^*$ transitions originating from the peptide group might be affected by membrane environments in which the dielectric constant is much lower than that for water.⁴¹

The secondary-structure contents were estimated using the DSSP program based on the numbers and positions of hydrogen bonds between peptide groups.⁴² The bends were treated as turns, and the 3_{10} -helices and the single residues assigned as turns and bends were classified as other structures. The contents of these secondary structures were estimated using the SELCON3 program, whose performance is comparable to those of the CDSSTR and CONTIN programs.³⁸ The numbers of α -helix and β -strand segments were calculated from the distorted α -helix and distorted β -strand contents, respectively.³⁹ The root-mean-square deviation (δ) and the Pearson correlation coefficient (r) for the correlation between the X-ray and VUVCD estimates of the secondary-structure contents for 31 reference proteins were 0.058 and 0.92, respectively.

Full details about secondary-structure analyses using VUVCD spectroscopy are available elsewhere.^{24, 25} The positions of α -helices and β -strands on the amino-acid sequence were predicted using the VUVCD-NN combination method, whose computational protocol is detailed elsewhere.^{43, 44} The turns and other structures estimated using the SELCON3 program were classified as ‘other structures’ in the VUVCD-NN combination method. The accuracy in predicting the positions of α -helices and β -strands was 75% for 30 reference proteins.⁴³

Results

The VUVCD spectra of AGP were measured from 260 to 170 nm using a VUVCD spectrophotometer in the N state at pH 7.4 and in the presence of DMPC, SM, DMPE, DMPS, and PI liposomes—corresponding to DMPC, SM, DMPE, DMPS, and PI states, respectively—at pH 4.5. The conformational differences of AGP between pH 7.4 and 4.5 would be minor since its secondary structures were found to be only slightly modified over the pH range from 10 to 4.5.^{18, 26} The VUVCD spectra for each liposome solution were also measured as the baseline, which was subtracted as the background from the spectra of mixtures of AGP and liposome. All of the VUVCD spectra including the baselines of liposome solutions were constant within an experimental error of 5% during data acquisition, which took about 1 hr. Thus, the obtained spectra are available for analyzing the liposome-induced conformational changes in AGP.

3.1 VUVCD spectra of membrane-bound states

Figure 2 shows the VUVCD spectra of AGP in the N state and the DMPC, SM, DMPE, DMPS, and PI states, which were obtained by subtracting the spectra of the glycan chain from the observed spectra of AGP, based on the weight proportion of protein and glycan in AGP as described previously²⁶ and in Figure S2.

The five phospholipid molecules used in this study (DMPC, SM, DMPE, DMPS, and PI) have characteristic head groups (Figure S1) located on the surface of the liposome because they have affinity to the hydrophilic region or aqueous solution, meaning that the molecular

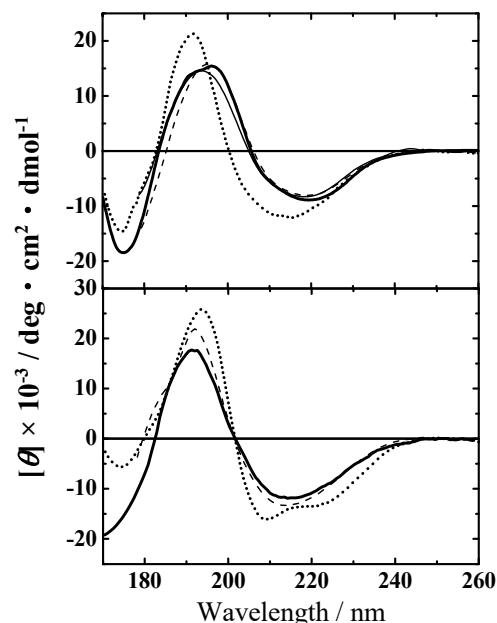


FIGURE 2 VUVCD spectra of AGP in the N state and the membrane-bound states at 25°C: (a) N state (thick line), DMPC state (thin line), SM state (dashed line), and DMPE state (dotted line), and (b) DMPS state (solid line), PI state (dotted line), and PI state for 1 M NaCl (dashed line). The solvents were 20 mM sodium phosphate buffer (pH 7.4) for the N state and 20 mM sodium acetate buffer (pH 4.5) for the membrane-bound states. A cell with a path length of 10.6 μ m was used for the measurements from 260 to 170 nm. All spectra were recorded with a 1.0-mm slit, a 4-s time constant, a 20-nm min^{-1} scan speed, and using four to nine accumulations.

characteristics of head groups such as differences in the net charge could affect the properties of the liposome surface.⁴⁵ The net charge of a liposome surface would be neutral in DMPC, SM, and DMPE because the negative charge in the phosphate group would be canceled by the positive charges of the choline of DMPC and SM and of the ethanolamine of DMPE. The DMPS and PI liposomes have negatively charged surfaces because the negative charge of the phosphate group could be retained due to the serine with zwitterions for DMPS and inositol without any charge for PI.

The VUVCD spectra of AGP in the N state and in the DMPC, SM, and DMPE states are shown in Figure 2a. The native AGP exhibited one positive peak at around 195 nm and two negative peaks around 220 and 175 nm, which are characteristic peaks of β -strand-rich proteins.^{24, 25} These characteristic peaks were mostly retained in the DMPC and SM states. However, the positions of peaks in the spectrum in the DMPE state were blue-shifted compared with those in the N, DMPC, and SM states, exhibiting two negative peaks around 215 and 175 nm and one positive peak near 190 nm as the CD intensity increased.

The VUVCD spectra of AGP in the DMPS and PI states are shown in Figure 2b. The DMPS state exhibited a spectrum similar to that

TABLE 1 Secondary-structure contents and numbers of segments of AGP in the N state and in the DMPC, SM, DMPE, DMPS, and PI states.

State	Percentage contents				Numbers of segments	
	α -Helix	β -Strand	Turn	Unordered	α -Helix	β -Strand
N state						
X-ray	18.0	39.3	15.9	26.8	4	9
VUVCD	17.2	37.8	22.7	23.1	4	11
Membrane-bound state						
DMPC	19.0	37.5	21.5	21.9	5	11
SM	18.1	40.4	21.0	21.4	4	11
DMPE	37.7	16.9	18.1	28.9	5	7
DMPS	28.9	18.6	21.4	30.9	6	6
PI	45.8	6.8	17.9	31.2	7	3
PI+NaCl	40.0	14.7	20.1	27.2	7	4

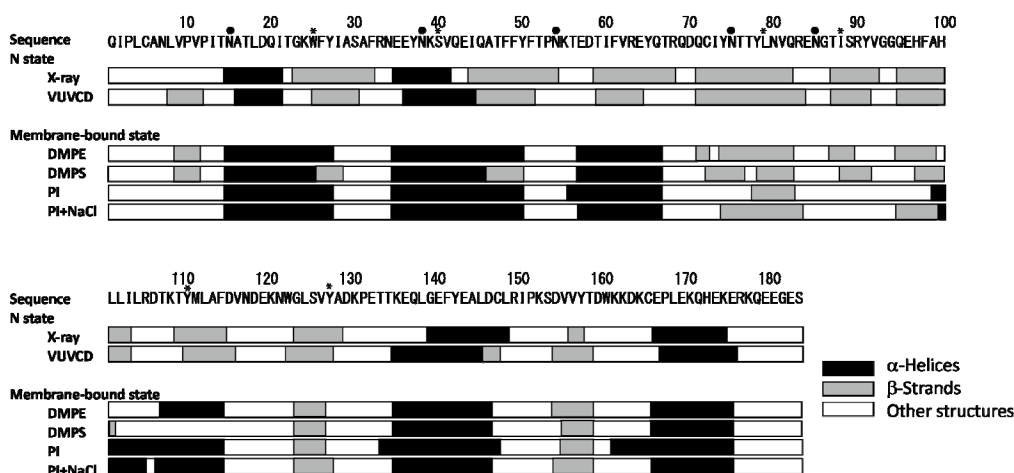


FIGURE 3 Sequence-based secondary structures of AGP in the N, DMPE, DMPS, and PI states predicted using the VUVCD-NN method. The sequence of native AGP was also estimated from X-ray data for comparison. The residues marked with filled circles (●) and asterisks (*) correspond to the glycan and predicted ligand-binding sites, respectively.

observed in the DMPE state, although the two spectra differed markedly below 180 nm. The PI state resulted in a large spectral change, showing three negative peaks at 222, 208, and 175 nm and a positive peak at 195 nm, which are characteristic of α -helix-rich proteins.^{24, 25} These spectral characteristics were similar to those found previously in the PG state.²⁶ To confirm the effect of oriented CD (OCD),⁴⁶ the CD spectrum of AGP in the PI state was measured from 260 to 198 nm with 200 μ m path length and compared that measured with 10.6 μ m path length as shown in Figure S3. Evidently, the both spectra were consistent in the overlap region, suggesting that the effect of OCD would be small or even negligible in the PI state. Thus, the spectra of AGP were highly dependent on the molecular characteristics of head groups of the constituent phospholipid molecules in the liposomes, which affected the conformations of AGP.

3.2 Secondary structures of membrane-bound states

The secondary-structure contents and numbers of segments of AGP in the N state and in the DMPC, SM, DMPE, DMPS, and PI states estimated from VUVCD spectra from 260 to 170 nm (Figure 2) are listed in Table 1. The results for the crystal structure are also listed in this table for comparison.¹⁴ The missing residues 176–183 in the crystal structure were considered as the unordered structures. The types of secondary structures in this study were determined using the DSSP method⁴² in which the 3_{10} -helices were assigned as unordered structures (see Materials and Methods).

As listed in Table 1, the contents of α -helices, β -strands, turns, and unordered structures of native AGP were 17.2%, 37.8%, 22.7%, and 23.1%, respectively, which were very similar to those found previously in the PG state²⁶ and for the crystal structure of unglycosylated recombinant AGP (18.0%, 39.3%, 15.9%, and 26.8%, respectively).¹⁴ This suggests that the effect of glycan chains on the secondary structures of AGP are small or even negligible. Further, 4 and 11 helix and strand segments, respectively, were found using VUVCD, with 4 and 9 found using X-ray crystallography, showing that combining the VUVCD method with the SELCON3 program³⁸ can successfully estimate the secondary-structure contents and numbers of segments of AGP in the N state.

The secondary-structure contents and numbers of segments in the DMPC and SM states are mostly consistent with those in the N state, as expected from the similarity of their VUVCD spectra. In the DMPE, DMPS, and PI states, it is evident that the contents of α -helices and β -strands uniquely increased and decreased, respectively, inducing the $\beta \rightarrow \alpha$ conformational change although the components of secondary structures differed among them (37.7% and 16.9%, respectively, in the DMPE state, 28.9% and 18.6% in the DMPS state, and 45.8% and 6.8% in the PI state). This suggests that the conformation of AGP is very sensitive to differences in the molecular characteristics of liposome surfaces.

3.3 Positions of secondary structures in membrane-bound states

VUVCD spectroscopy itself provides no information about the sequences of the secondary structures in principle, and hence an algorithm exploiting the correlations between the secondary structures (α -helices, β -strands, and other structures) and amino-acid sequences of many proteins whose X-ray structures have been resolved is necessary. The present study utilized the NN algorithm of Jones⁴⁴ since it was technically convenient to combine with VUVCD data.

Figure 3 shows the positions of α -helices, β -strands, and other structures of AGP in the N state and in the DMPE, DMPS, and PI states predicted by the VUVCD-NN method, together with the N state as determined from X-ray data. The secondary-structure sequences in the DMPC and SM states are not shown in this figure because they were similar to those in the N state. We first compared the sequence data between the VUVCD and X-ray estimates. Four helical segments in the N state estimated by the VUVCD-NN method were assigned as residues 16–21, 36–44, 135–145, and 167–175; these helical segments corresponded to residues 15–21, 35–41, 139–148, and 166–174, respectively, identified in the X-ray data. Further, the positions of β -strands other than the N-terminal strand (residues 8–10) were also consistent with the results from the X-ray data, resulting in a total prediction accuracy of the sequences between the X-ray and VUVCD-NN estimates in the N state of 80% in terms of the success rate (quantified as the Q_3 value).⁴⁷ These results suggest that the VUVCD-NN method used in this study would be a useful tool for monitoring the conformational changes in AGP induced by the addition of liposomes.

The DMPE, DMPS, and PI states had characteristic conformations consisting of some long α -helices and small β -strands (Figure 3). The positions of six α -helix segments in the DMPE state were assigned as residues 15–27, 35–50, 57–66, 107–114, 135–146, and 166–175, which are denoted as A-, B-, C-, D-, E-, and F-helices, respectively. The positions of five α -helices in the DMPS state were assigned as residues 15–25, 35–46, 57–66, 135–146, and 166–175, which are denoted as A-, B-, C-, E-, and F-helices, respectively. Further, the regions of six α -helices in the PI state were assigned as residues 15–27, 35–50, 56–66, 99–114, 133–147, and 161–175, which are denoted as A-, B-, C-, D-, E-, and F-helices, respectively. These results suggest that the AGP formed characteristic conformations depending on the liposomes, although the A-, B-, C-, and E-helix segments were in similar positions among the three states. It is unclear whether these helical formations were affected by five glycan chains linked to Asn-15, -38, -54, -75, and -85, but the types of secondary structures at these linkage sites were mostly conserved in the conformational changes in AGP (Figure 3). The numbers of segments predicted at the sequence level did not necessarily agree with those predicted from VUVCD data because sequence-alignment minimization was performed in the VUVCD-NN method.⁴³

The weights of 20 amino acids investigated in this study were calculated without considering their solvent dependence because the

intrinsic solvent dependence is generally difficult to evaluate. However, since VUVCD spectroscopy can predict the secondary-structure contents and segments much more accurately than can NN analysis,⁴³ the effects of the solvent on the weights would introduce only small errors into sequence predictions made using the VUVCD-NN method. Actually, the predictive accuracy of sequences of secondary structures of 15 membrane proteins were 73% (data not shown). Therefore, the VUVCD-NN method would be valuable for predicting the sequences of secondary structures of a peripheral membrane protein such as AGP, and useful for characterizing the conformation of AGP depending on the types of liposomes, which are crucial factors for understanding the membrane interaction sites and the mechanism of interaction between AGP and lipid membranes.

Discussion

This study found that the VUVCD spectra of AGP in the N state and in the DMPE, DMPS, and PI states (Figure 2) provided detailed information about the secondary structures, in terms of not only the contents and numbers of segments (Table 1) but also their positions on the amino-acid sequence (Figure 3). Although this secondary-structure information could not be used to determine the tertiary structure of the membrane-bound conformation of AGP and the liposomes used in this study were model membranes constructed from simple phospholipid molecules, the structural data of membrane-bound AGP including the positions of secondary structures can be used in discussions of the membrane interaction sites and the mechanism of interaction between AGP and lipid membranes at the sequence level.

Knowledge of the membrane interaction sites of AGP is important for understanding the mechanism of interaction between AGP and lipid membranes. Previous studies^{9, 26} found that the N- and C-terminal helices in the PG state, which are residues 15–27 and 161–175, respectively, are candidate sites for the interactions. In the present study the two helices at the N- and C-terminals were designated as A- and F-helices, respectively. The A-helix in the N state was markedly extended in the three states (residues 15–25 or 26), but the F-helix was only extended in the PI state (residues 161–175). We examined the characteristics of A- and F-helices in the DMPE, DMPS, and PI states to confirm the possibility of them acting as interaction sites. The net charges of the A- and F-helices were calculated to be 0 and –1, respectively, for DMPE, 0 and –1 for DMPS, and 0 and +1 for PI, based on the numbers of acidic (Asp and Glu) and basic (Lys, Arg, and His) residues in each helix segment. These net charges would increase slightly because the carboxyl groups of Asp and Glu residues ($pK_a \approx 4$) are not completely ionized at pH 4.5. Further, according to the HELIQUEST program,⁴⁸ the A-helix segments in the three states comprised the localized polar and nonpolar surfaces as seen in the amphiphilic helix, indicating that the localized nonpolar surface could interact with the hydrophobic moiety of the membrane. Further, the F-helix had a positively charged region in the PI state, suggesting that the negatively charged liposome surface would interact with the positively charged F-helix in that state. These results indicate that the candidate membrane interaction sites would be the amphiphilic A-helix in the DMPE, DMPS, and PI states and the positively charged F-helix in the PI state. Another candidate would be the D-helix (residues 99–114) in the PI state because this region had a positive net charge, which could induce an interaction with the negatively charged liposome and moreover half of all of the residues of this helix are hydrophobic amino acids. However, this region comprises a core with a β -barrel conformation in native AGP, which might make it difficult to interact directly with the liposome. It is likely that the region of the D-helix in the PI state would form a helical structure after the A- and F-helices interacted with the liposome.

As mentioned above, AGP includes three Trp residues (W25, W122, and W160) (Figure 1), and W25 and W160 are known to be crucial residues for membrane interactions in the PG state.⁹ W25 is the constituent residue of A-helices in the DMPE, DMPS, and PI states, while only W160 is involved with the F-helix in the PI state. To characterize the two membrane interaction sites (A- and F-helix regions), we investigated the effect of salt on the conformation of AGP in the DMPE, DMPS, and PI states. The VUVCD spectra of AGP in

the DMPE, DMPS, and PI states in the presence of 1 M sodium chloride (NaCl) are presented in Figure S4 (DMPE and DMPS states) and Figure 2b (PI state). Spectral changes were not observed in the DMPS and DMPE states but they were observed in the PI state. It was particularly interesting that the spectrum in the PI state for the NaCl solution was similar to those in the DMPE and DMPS states. Salt is known to reduce the electrostatic interactions between proteins and membranes,^{49–51} implying that the electrostatic interaction exists in the PI state.

The positions of conformational changes in the PI state due to the addition of NaCl were addressed by predicting the secondary-structure sequence, as shown in Figure 3. It is evident that the F-helix shortened in the PI state to have the same length as in the DMPE and DMPS states. This result is reasonable given that the F-helix involved in W160 would be expected to interact with the liposome surface via electrostatic interactions and that the addition of salt would reduce this interaction. Similar results were obtained in the fluorescence spectra, in which the position of the peak in the PI state was blue-shifted compared with that in the DMPE state, but the peak returned to the positions in the DMPE state when NaCl was added to the PI state (Figure S5), directly reflecting the change in the environment around W160.⁵² Further, the length of A-helix including W25 was maintained in the PI states with 1 M NaCl, which is probably due to the amphiphilic A-helix strongly interacting with the liposome surface via hydrophobic interactions.

Based on these characteristics of the membrane interaction sites of AGP, this protein has at least two interaction sites with membrane: the amphiphilic A-helix and the positively charged F-helix. It is known that the protein–membrane interactions mainly comprise electrostatic interactions between the anionic head groups of lipids and the positively charged protein or regions of protein and the subsequent penetration of some hydrophobic regions of the protein into the membrane.⁵³ However, as mentioned above, although the DMPC, SM, and DMPE liposomes have a neutral net charge on their surface, the membrane interaction of AGP was induced only in the DMPE state.

Phosphatidylethanolamine (PE) contains an ethanolamine head group rather than the choline one present in phosphatidylcholine and SM. It is reported that this substitution changes many properties of the phospholipid. Litzinger and Huanget showed that one of the main differences between dioleoyl phosphatidylethanolamine (DOPE) and dioleoyl phosphatidylcholine (DOPC) is that DOPE tends to forming nonbilayer structures, such as in the hexagonal H_{II} phase, whereas this activity is absent in DOPC.⁵⁴ This effect of not forming a bilayer in DOPE can decrease the head-group pressure and allow a peripheral membrane protein to access the inside of the liposome, which contains a negatively charged phosphate group.⁵⁵ Although the effect of not having a bilayer might be small at 25°C because the hexagonal H_{II} phase in the mixture of dielaidoyl PE and DOPE constituted 100% of the population at 50°C but this decreased to about 10% at 25°C,⁵⁶ AGP might weakly interact with the nonrigid surface of the PE liposome via interactions between the positively charged AGP and the negatively charged internal phosphate group.

PI includes myoinositol in its head group, which has six hydroxyl groups (Figure S1) with a strong affinity to aqueous solutions. Nishi et al. investigated the conformation of AGP at pH 4.0 in various alcohol solutions as a membrane-mimicking environment, and found that the hydroxyl group of the alcohol only plays a role in the dissolution in water and that the formation of α -helix is induced by the hydrocarbon moiety.⁵⁷ Although alcohol and inositol molecules have markedly different structures, it seems that the hydroxyl group itself does not contribute to the helical conformation, meaning that the negative charged liposome surface contributed strongly to the conformational changes in AGP in the PI state. On the other hand, the DMPS and PI liposomes should have negatively charged surfaces but they induced different conformations. Moncelli et al. suggested that the charge density of the phosphatidylserine (PS) lipid film changed from slight negative to slight positive values over the pH range from 7.5 to 3 due to the anomalous behavior of the phosphate group.⁵⁸ Therefore, the effect of the negative net charge of the PS liposome is reduced in a mildly acidic condition (pH 4.5) compared to that of the PI liposome. These slight differences in the net charge might induce differences in the conformations between the DMPS and PI states.

Thus, the physical properties of each of the DMPE, DMPS, and PI liposomes are very complicated and depend on the experimental conditions, but their individual uniqueness would induce characteristic membrane-bound conformations in the three states. However, it is conceivable that the interaction mechanism would be similar among the DMPE, DMPS, and PI states because all three states formed A-helix segments but there would be an additional step in the PI state. In the DMPE and DMPS states, the positively charged AGP molecule (pI=2.8–3.8) approaches the anionic regions in the membrane surface via an electrostatic interaction and the A-helix region including W25 is formed on the membrane surface via the hydrophobic interaction, followed by the formation of other helices. In the PI state, in addition to the interaction processes and the formation of A-helix observed in the DMPE and DMPS states, the F-helix region near W160 was formed weakly in contact with the membrane surface via the electrostatic interaction, followed by the formation of other helices. From the viewpoint of the protein-mediated uptake mechanism of drugs, the formation and extension of A-helix would be crucial for releasing neutral drugs because W25 is known to be the most-important site for binding with drugs such as progesterone via the molecular docking and the induced CD spectra of drug-AGP complex (Figure 3).^{14, 59} These unique interaction mechanisms are still speculative and it might be difficult to confirm further experimentally. However, additional techniques for investigating membrane interactions such as fluorescence quenching,⁵² mass spectroscopy,⁶⁰ and site-directed spin labeling and electron paramagnetic resonance spectroscopy⁶¹ could also be useful for elucidating more details about the mechanism of interaction between AGP and cell membranes.

Conclusions

This study applied VUVCD spectroscopy to characterize the secondary structures of AGP in the N and membrane-bound states. A comprehensive analysis of the contents, numbers of segments, and sequences of the secondary structures revealed that the membrane-bound conformation of AGP is strongly depending on the types of constituent phospholipid molecules in the liposomes. These results represent important information for understanding the membrane interaction sites and the mechanism of interaction between AGP and lipid membranes, in which at least the amphiphilic N-terminal helix and the positively charged C-terminal helix in the membrane-bound conformation would be candidates for the interaction sites with the membrane surface, with the two helices interacting with the membrane via hydrophobic and electrostatic interactions, respectively. These results further demonstrate that VUVCD spectroscopy is a useful tool for characterizing the mechanism of interaction between AGP and lipid membranes, and could contribute to knowledge of the structural biology of membrane-bound proteins such as the integral and nonintegral membrane proteins, especially for targets that are not amenable to X-ray and NMR analyses.

Acknowledgements

This work was financially supported by Grants-in-Aid for Scientific Research from the Ministry of Education, Culture, Sports, Science, and Technology of Japan (numbers 19K06587 and 15K07028). The measurements of vacuum-ultraviolet circular-dichroism spectra were carried out with the approval of the Hiroshima Synchrotron Radiation Center of Hiroshima University (proposal numbers 18AG012, 17AG005, and 16AG009).

Supporting information

Chemical structures of head groups of DMPC, SM, DMPE, DMPS, and PI (Figure S1), VUVCD spectra of AGP with and without glycan chains at pH 7.4 (Figure S2), CD spectra of AGP in the PI state measured with 10.6 μm and 200 μm path-length cell (Figure S3). VUVCD spectra of AGP in the DMPE and DMPS states in the presence or absence of 1M NaCl (Figure S4), and the fluorescence spectra of AGP in the N state and in the DMPE, DMPS, and PI states (Figure S5).

REFERENCES AND NOTES

- Catterall WA. Voltage-gated sodium channels at 60: structure, function and pathophysiology. *J Physiol.* 2012;590:2577–2589.
- Bourne HR. How receptors talk to trimeric G proteins. *Curr Opin Cell Biol.* 1997;9:134–142.
- Torres GE, Gainetdinov RR, Caron MG. Plasma membrane monoamine transporters: structure, regulation and function. *Nat Rev Neurosci.* 2003;4:13–25.
- Lesieur C, Vécsey-Semjén B, Abrami L, Fivaz M, Gisou van der Goot F. Membrane insertion: the strategies of toxins. *Mol Membr Biol.* 1997;14:45–64.
- Ow YLP, Green DR, Hao Z, Mak TW. Cytochrome c: functions beyond respiration. *Nat Rev Mol Cell Biol.* 2008;9:532–542.
- Selkoe JD. Folding proteins in fatal ways. *Nature.* 2003;426:900–904.
- Matsumoto K, Sukimoto K, Nishi K, Maruyama T, Suenaga A, Otagiri M. Characterization of ligand binding sites on the alpha1-acid glycoprotein in humans, bovines and dogs. *Drug Metab Pharmacokinet.* 2002;17:300–306.
- Ganguly M, Carnigha, RH, Westphal U. Steroid-protein interactions. XIV. Interaction between human alpha 1-acid glycoprotein and progesterone. *Biochemistry.* 1967;6:2803–2814.
- Nishi K, Maruyama T, Halsall HB, Handa T, Otagiri M. Binding of alpha1-acid glycoprotein to membrane results in a unique structural change and ligand release. *Biochemistry.* 2004;43:10513–10519.
- Weisiger R, Gollan J, Ockner R. Receptor for albumin on the liver cell surface may mediate uptake of fatty acids and other albumin-bound substances. *Science.* 1981;211:1048–1051.
- Fournier T, Medjoubi-N N, Porquet D. Alpha-1-acid glycoprotein. *Biochim Biophys Acta.* 2000;1482:157–171.
- Bayard B, Fournet B. Hydrazinolysis and nitrous acid deamination of the carbohydrate moiety of alpha1-acid glycoprotein. *Carbohydr Res.* 1976;46:75–86.
- Halsall HB, Austin RC, Dage JL, Sun H, Schlueter KT. Structural aspects of alpha1-acid glycoprotein and its interaction. In *Proceedings of the International Symposium on Serum Albumin and Alpha1-acid Glycoprotein* (Otagiri M, Sugiyama Y, Testa B, Tillement JP, Eds.), Tokyo Print, Kumamoto, Japan; 2000:45–54.
- Schönfeld DL, Ravelli RB, Mueller U, Skerra A. The 1.8-Å crystal structure of alpha1-acid glycoprotein (Orosomucoid) solved by UV RIP reveals the broad drug-binding activity of this human plasma lipocalin. *J Mol Biol.* 2008;384:393–405.
- Eisenberg DS, Sawaya MR. Structural studies of amyloid proteins at the molecular level. *Annu Rev Biochem.* 2017;86:69–95.
- Nishi K, Sakai N, Komine Y, Maruyama T, Halsall HB, Otagiri M. Structural and drug-binding properties of alpha(1)-acid glycoprotein in reverse micelles. *Biochim Biophys Acta.* 2002;1601:185–191.
- Kopecký V Jr, Ettrich R, Hofbauerová K, Baumruk V. Structure of human alpha1-acid glycoprotein and its high-affinity binding site. *Biochem Biophys Res Commun.* 2003;300:41–46.
- Scirè A, Baldassarre M, Lupidi G, Tanfani F. Importance of pH and disulfide bridges on the structural and binding properties of human alpha1-acid glycoprotein. *Biochimie.* 2011;93:1529–1536.
- Lupidi G, Camaioni E, Khalifé H, Avenali L, Damiani E, Tanfani F, Scirè A. Characterization of thymoquinone binding to human alpha1-acid glycoprotein. *J Pharm Sci.* 2012;101:2564–2573.
- Johannessen C, Pendrill R, Widmalm G, Hecht L, Barron LD. Glycan structure of a high-mannose glycoprotein from Raman optical activity. *Angew Chem Int Ed Engl.* 2011;50:5349–5351.
- Kopecký V Jr, Ettrich R, Pazderka T, Hofbauerová K, Řeha D, Baumruk V. Influence of ligand binding on structure and thermostability of human alpha1-acid glycoprotein. *J Mol Recognit.* 2016;29:70–79.
- Fasman GD. *Circular Dichroism and the Conformational Analysis of Biomolecules.* Plenum Press, NY; 1996.

23. Nishi K, Komine Y, Fukunaga N, Maruyama T, Suenaga A, Otagiri M. Involvement of disulfide bonds and histidine 172 in a unique beta-sheet to alpha-helix transition of alpha 1-acid glycoprotein at the biomembrane interface. *Proteins*. 2006;63:611–620.
24. Matsuo K, Yonehara R, Gekko K. Secondary-structure analysis of proteins by vacuum-ultraviolet circular dichroism spectroscopy. *J Biochem*. 2004;135:405–411.
25. Matsuo K, Yonehara R, Gekko K. Improved estimation of the secondary structures of proteins by vacuum-ultraviolet circular dichroism spectroscopy. *J Biochem*. 2005;138:79–88.
26. Matsuo K, Namatame H, Taniguchi M, Gekko K. Membrane-induced conformational change of alpha1-acid glycoprotein characterized by vacuum-ultraviolet circular dichroism spectroscopy. *Biochemistry*. 2009;48:9103–9111.
27. Zhang X, Ge N, Keiderling TA. Electrostatic and hydrophobic interactions governing the interaction and binding of beta-lactoglobulin to membranes. *Biochemistry*. 2007;46:5252–5260.
28. Muruganandam G, Bürck J, Ulrich AS, Kursula I, Kursula P. Lipid membrane association of myelin proteins and peptide segments studied by oriented and synchrotron radiation circular dichroism spectroscopy. *J Phys Chem B*. 2013;117:14983–14993.
29. Marcus AJ, Ullman HL, Safier LB. Lipid composition of subcellular particles of human blood platelets. *J Lipid Res*. 1969;10:108–114.
30. Pace CN, Vajdos F, Fee L, Grimsley G, Gray T. How to measure and predict the molar absorption coefficient of a protein. *Protein Sci*. 1995;4:2411–2423.
31. Silvius JR. Thermotropic phase transitions of pure lipids in model membranes and their modifications by membrane proteins. In *Lipid-Protein Interactions* (Jost PC, Griffith OH, Eds), John Wiley, New York; 1982:239–281.
32. Koynova R, Caffrey M. Phases and phase transitions of the sphingolipids. *Biochim Biophys Acta*. 1995;1255:213–236.
33. O'Neill SD, Leopold AC. An assessment of phase transitions in soybean membranes. *Plant Physiol*. 1982;70:1405–1409.
34. Ojima N, Sakai K, Matsuo K, Matsui T, Fukazawa T, Namatame H, Taniguchi M, Gekko K. Vacuum-ultraviolet circular dichroism spectrophotometer using synchrotron radiation: optical system and on-line performance. *Chem Lett*. 2001;30:522–523.
35. Matsuo K, Sakai K, Matsushima Y, Fukuyama T, Gekko K. Optical cell with a temperature-control unit for a vacuum-ultraviolet circular dichroism spectrophotometer. *Anal Sci*. 2003;19:129–132.
36. Matsuo K, Maki Y, Namatame H, Taniguchi M, Gekko K. Conformation of membrane-bound proteins revealed by vacuum-ultraviolet circular-dichroism and linear-dichroism spectroscopy. *Proteins*. 2016;84:349–359.
37. Wallace BA, Lees J, Orry AJW, Lobley A, Janes RW. Analyses of circular dichroism spectra of membrane proteins. *Protein Sci*. 2003;12:875–884.
38. Sreerama N, Woody RW. Estimation of protein secondary structure from circular dichroism spectra: comparison of CONTIN, SELCON, and CDSSTR methods with an expanded reference set. *Anal Biochem*. 2000;287:252–260.
39. Sreerama N, Venyaminov SY, Woody RW. Estimation of the number of alpha-helical and beta-strand segments in proteins using circular dichroism spectroscopy. *Protein Sci*. 1999;8:370–380.
40. Sreerama N, Woody RW. On the analysis of membrane protein circular dichroism spectra. *Protein Sci*. 2004;13:100–112.
41. Park K, Perczel A, Fasman GD. Differentiation between transmembrane helices and peripheral helices by the deconvolution of circular dichroism spectra of membrane proteins. *Protein Sci*. 1992;1:1032–1049.
42. Kabsch W, Sander C. Dictionary of protein secondary structure: pattern recognition of hydrogen-bonded and geometric features. *Biopolymers*. 1983;22:2577–2637.
43. Matsuo K, Watanabe H, Gekko K. Improved sequence-based prediction of protein secondary structures by combining vacuum-ultraviolet circular dichroism spectroscopy with neural network. *Proteins*. 2008;73:104–112.
44. Jones DT. Protein secondary structure prediction based on position-specific scoring matrices. *J Mol Biol*. 1999;292:195–202.
45. Patil YP, Jadhav S. Novel methods for liposome preparation. *Chem Phys Lipids*. 2014;177:8–18.
46. Bürck J, Wadhwani P, Fanghänel S, Ulrich AS. Oriented circular dichroism: a method to characterize membrane-active peptides in oriented lipid bilayers. *Acc. Chem. Res*. 2016;49:184–192.
47. Kabsch W, Sander C. How good are predictions of protein secondary structure? *FEBS Lett*. 1983;155:179–182.
48. Gautier R, Douguet D, Antonny B, Drin G. HELIQUEST: a web server to screen sequences with specific alpha-helical properties. *Bioinformatics*. 2008;24:2101–2102.
49. Zhai J, Wooster TJ, Hoffmann SV, Lee TH, Augustin MA, Aguilar MI. Structural rearrangement of beta-lactoglobulin at different oil-water interfaces and its effect on emulsion stability *Langmuir*. 2011;27:9227–9236.
50. Mo H, Tay KG, Ng HY. Fouling of reverse osmosis membrane by protein (BSA): effects of pH, calcium, magnesium, ionic strength and temperature. *J Membr Sci*. 2008;315:28–35.
51. Zhao Y, Li F, Carvajal MT, Harris MT. Interactions between bovine serum albumin and alginate: an evaluation of alginate as protein carrier. *J Colloid Interface Sci*. 2009;332:345–353.
52. Gorbenko GP, Ioffe VM, Kinnunen PKJ. Binding of lysozyme to phospholipid bilayers: evidence for protein aggregation upon membrane association. *Biophys J*. 2007;93:140–153.
53. Cornell DG, Patterson D. Interaction of phospholipids in monolayers with beta-lactoglobulin adsorbed from solution. *J Agric Food Chem*. 1989;37:1455–1459.
54. Litzinger D, Huang L. Phosphatidylethanolamine liposomes: drug delivery, gene transfer and immunodiagnostic applications. *Biochim Biophys Acta*. 1992;1113:201–227.
55. van den Brink-van der Laan E, Killian JA, de Kruijff B. Nonbilayer lipids affect peripheral and integral membrane proteins via changes in the lateral pressure profile. *Biochim Biophys Acta*. 2004;1666:275–288.
56. Van Echteld CJA, Van Stigt R, De Kruijff B, Leunissen-Bijvelt J, Verkley AJ, De Gier J. Gramicidin promotes formation of the hexagonal H_{II} phase in aqueous dispersions of phosphatidylethanolamine and phosphatidylcholine. *Biochim Biophys Acta*. 1981;648:287–291.
57. Nishi K, Komine Y, Sakai N, Maruyama T, Otagiri M. Cooperative effect of hydrophobic and electrostatic forces on alcohol-induced alpha-helix formation of alpha1-acid glycoprotein. *FEBS Lett*. 2005;17:3596–3600.
58. Moncelli MR, Becucci L, Guidelli R. The intrinsic pK_a values for phosphatidylcholine, phosphatidylethanolamine, and phosphatidylserine in monolayers deposited on mercury electrodes. *Biophys J*. 1980;66:1969–1980.
59. Zsila F, Iwao Y. The drug binding site of human alpha1-acid glycoprotein: Insight from induced circular dichroism and electronic absorption spectra. *Biochim Biophys Acta*. 2007;1770:797–809.
60. Yamamoto T, Izumi S, Gekko K. Mass spectrometry on hydrogen/deuterium exchange of dihydrofolate reductase: effects of ligand binding. *J Biochem*. 2004;135:663–671.
61. Homchaudhuri L, Polverini E, Gao W, Harauz G, Boggs JM. Influence of membrane surface charge and post-translational modifications to myelin basic protein on its ability to tether the Fyn-SH3 domain to a membrane in vitro. *Biochemistry*. 2009;48:2385–2393.

Graphical Abstract

